International Journal for Modern Trends in Science and Technology
Volume 9, Issue 08, pages 80-88
ISSN: 2455-3778 online
Available online at: http://www.ijmtst.com/vol9issue09.html
DOI: https://doi.org/10.46501/IJMTST0909014

Control of Permanent Magnet Synchronous Motor Drive for Solar Water Pumping Systems using Artificial Neural Networks

B. Sridhar[1] | Dr. K. Siva Kumar[2] | M. Harish[3]

[1]Department of EEE, Sri Venkatesa Perumal College of Engineering and Technology, Puttur, Andhrapradesh, India
[2]Department of EEE, Sri Venkatesa Perumal College of Engineering and Technology, Puttur, Andhrapradesh, India
[3]Department of EEE, Sri Venkatesa Perumal College of Engineering and Technology, Puttur, Andhrapradesh, India

To Cite this Article
B. Sridhar, Dr. K. Siva Kumar and M. Harish. Development of a Multifunctional Non-Isolated Dual Input-Dual Output Converter using Advanced Controller for Electric Vehicle Applications, 2023, 9(09), pages. 80-88.https://doi.org/10.46501/IJMTST0909014

Article Info
Received: 28 August 2023; Accepted: 20 September 2023; Published: 24 September 2023.

ABSTRACT

In this paper a new ANN-based control system for a Permanent Magnet Synchronous Motor (PMSM) drive in solar water pumping systems integrated with INC-MPPT are compared. Remote and off-grid locations need solar water pumping devices for sustainable water solutions. For energy efficiency, water reliability, and solar energy harvesting, PMSM drive control must be efficient. The current control system uses a fuzzy controller with heuristic decision-making. The suggested control system uses an ANN instead of a fuzzy controller to tune control parameters based on real-time solar radiation, water demand, and system efficiency. ANNs give more flexibility without unclear rules. We simulate and assess both control systems using MATLAB Simulink to compare their energy efficiency, maintenance needs, system dependability, and adaptability to changing environmental conditions and system dynamics. Simulations show that the ANN-based control system outperforms the fuzzy controller in optimizing PMSM drive performance, reducing energy consumption, and maintaining water supply. This study shows the benefits of using INC-MPPT to switch from heuristic-based to data-driven ANN control. Such a change may boost solar water pumping system performance and make them sustainable for off-grid and distant use.

KEYWORDS: Solar Water Pumping, Permanent Magnet Synchronous Motor, Fuzzy Logic Control, ANN Control, Maximum Power Point Tracking, Boost Converter, Voltage Source Inverter.

1. INTRODUCTION

Highlight In an era of escalating power demand and declining conventional energy sources, renewable energy (RE) sources provide promising solutions for filling the rapidly expanding gap between energy need and supply. In addition, since they cut down on carbon dioxide production, RE sources provide a practical approach to fighting climate change. Growing our dependence on renewable energy is an important step towards global sustainability. Several groups in the

public sector, the academic community, and the electric power sector are working to increase the use of RE sources. The sun is one of the most abundant and accessible renewable energy sources, but it is far from the sole option. Solar energy has a wide range of potential uses. We urge wider adoption and usage of solar photovoltaic (PV) producing systems as their price continues to reduce [1-2]. Solar water pumping is a new use for photovoltaic (PV) generating systems [3]. Particularly useful are off-grid locations with access to sufficient sunshine. It would help improve people's standard of life by addressing their most basic need: for water. Furthermore, it would encourage industrial and agricultural growth in rural areas [4]. Electric motors are required to power pumps in solar-powered systems. Solar water pumps employ both direct current (DC) and alternating current (AC) drivers [5-9]. Wear on the brush and commutator assembly is a significant issue for DC motors used in solar-powered water pumping systems [5]. Since induction motors are low-cost and dependable, they are often utilised in AC motor-driven solar water pumping systems [6]. However, because to its lower efficiency and increased reactive power need, it is quite inefficient for this application [7]. Larger solar photovoltaic arrays are required for lower efficiency levels. Permanent magnet synchronous motors (PMSMs) [8] are a great solution to these issues. Due to its high efficiency, high power density, strong power factor, and superior dynamic performance compared to other electric drives [8-10], PMSM is particularly applicable for solar water pumping. Vector control and direct torque control (DTC) are the most often used approaches for adjusting PMSM speeds [11]. DTC simplifies and expedites the process of controlling speed by separating the control of torque and flux. Also considered are torque and flux ripple [12]. Direct-axis and quadrature-axis components of the stator currents are isolated and regulated as field and armature current in a vector-controlled DC motor for a more immediate reaction to speed changes [13]. The proportional integral (PI) controller is often used for velocity regulation due to its simplicity. However, the PMSM drive's nonlinearity implies that excellent dynamic performance cannot be guaranteed by the PI controller. Many non-linear control strategies have been presented in the current literature to deal with these issues, such as sliding mode control [14], artificial intelligence control [15-16], robust control [17], adaptive control [18], backstepping control [19], and so on. Each of the aforementioned techniques improves system performance, although some are easier to execute than others. However, most of them won't do their jobs unless you adjust certain parameters. Artificial intelligence techniques, as reported in the literature, improve the dynamic performance of nonlinear systems while also making them less sensitive to changes in their parameters. Artificial neural networks (ANNs) are among the most widely used AI systems at present [15]. The present control system makes use of a fuzzy controller, which relies on heuristic criteria for decision-making. Instead of using a fuzzy controller, as is often done, the proposed control system makes use of an artificial neural network (ANN), allowing for the adaptive tuning of control parameters in real time in response to changes in solar radiation, water demand, and system efficiency (see Fig. 1). The ANN may be trained without the use of predetermined fuzzy rules, making it more flexible. Using MATLAB Simulink, we model and comprehensively evaluate both control systems, allowing for a direct comparison of their abilities to deal with energy consumption, maintenance, system dependability, and response to changes in both the external environment and the system's internal dynamics. For a solar PV integrated system to operate at peak efficiency, maximum power point tracking (MPPT) must be used. Numerous talks and presentations have already covered MPPT techniques. The open- and closed-circuit voltage and current relationship is used by the simplest MPPT techniques. However, their tracking abilities are subpar. Both the incremental conductance (INC) and perturb and observe (P&O) methods of maximum power point tracking (MPPT) have been shown to have very high tracking efficiencies. Many systems based on optimisation approaches, such as neural networks, evolutionary algorithms, fuzzy logic, Grey Wolf optimisation, particle swarm optimisation, etc., have shown excellent tracking efficacy even in the presence of partial shade [20]. When comparing the two widely used algorithms, P&O is the easier to implement. Unfortunately, it has a steady-state oscillation and drift problem. Although INC is a challenging method for MPPT, the results are impressive in both static and dynamic conditions. This research presents a solar

water pumping system that is powered by a photovoltaic (PV) array and is operated by a permanent magnet synchronous motor (PMSM). The proposed architecture employs a hybrid PI controller for PMSM speed regulation and INC-based MPP tracking to maximise power harvesting from a solar PV array. The hybrid PI controller incorporates both an ANN and a PI controller. The ANN performs corrections, as shown in Fig. 1, based on the magnitude and direction of the speed error. The PMSM's speed is controlled by the PI controller, which receives inputs for both the modified error and the speed error. The supplied controller improves the dynamic and steady-state reactivity of the solar water pumping system. We model and simulate the whole system, including the proposed controller, using the MATLAB/Simulink Simscape Sim power system toolbox. The DS-1004 is a digital signal processor (DSP)-based controller used to validate the simulation findings experimentally. The starting, steady-state, and even solar insolation fluctuation behaviour of the system are all investigated to help put it in perspective.

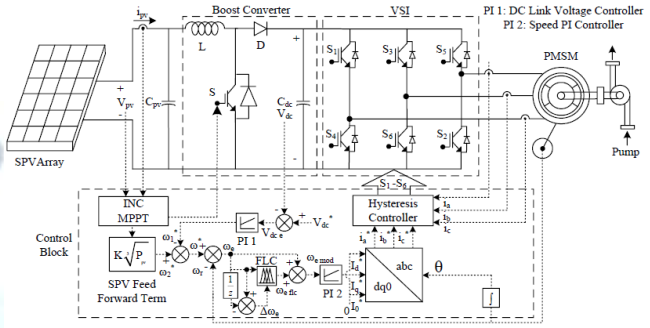

Fig. 1 Existing configuration for solar water pumping system.

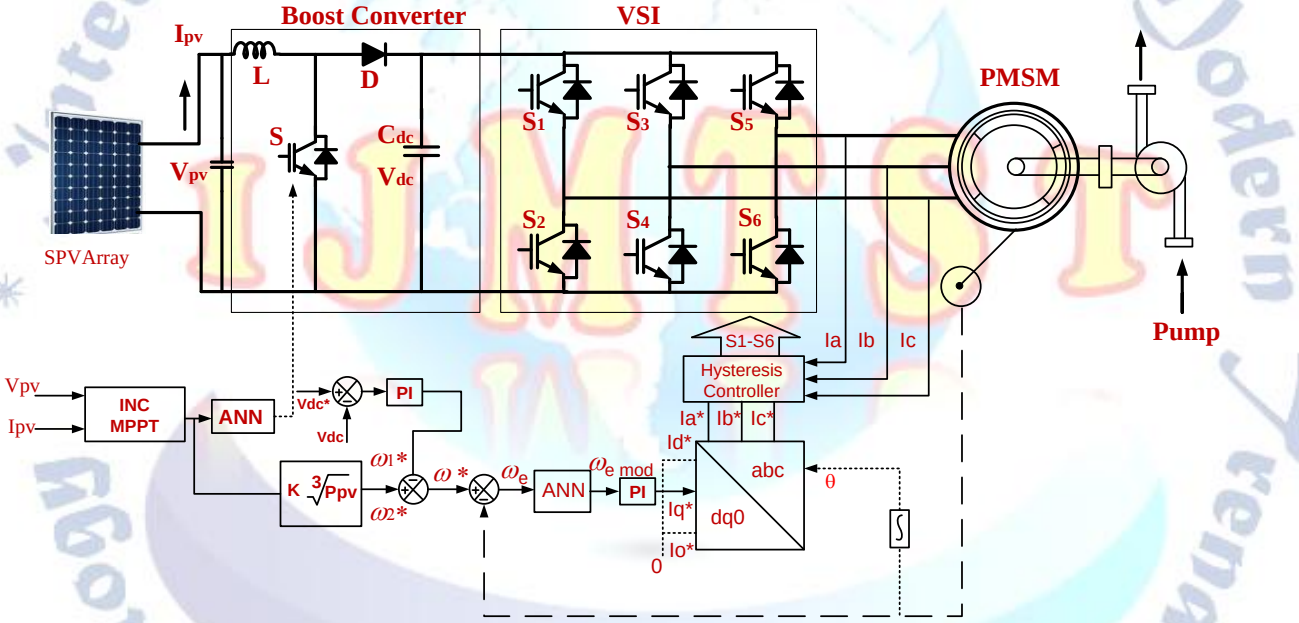

Fig. 2 proposed configuration for solar water pumping system.

2. SYSTEM OPERATION AND DESIGN

This page describes the solar panels, the DC-DC boost converter, the voltage source inverter (VSI) based on three-phase insulated gate bipolar transistors (IGBTs), the permanent magnet synchronous motor (PMSM), and the pump. The solar PV array uses the sunshine to generate power. This current is sent into the input of a DC-DC boost converter. By adjusting the duty ratio, the boost converter keeps the solar PV array's voltage at its MPP. The output of the boost converter supplies power to the VSI. This is the energy that drives the PMSM after being processed by the VSI. The PMSM's converted mechanical rotational energy spins the pump that is mechanically linked to the PMSM. When the pump is in motion, water is pumped. Regulation is the subject of much criticism. The presented architecture includes a solar PV array, DC - DC boost converter, and pump in the proper proportions to allow pumping to occur despite low levels of insolation. In what follows, we'll examine how various components of the system were built.

3. MODELING OF PROPOSED SYSTEM CONFIGURATION

A. Modeling of solar PV System

The voltage/current characteristic equation for a solar cell with a light source and a diode is shown in Fig. 3. Connecting solar cells in series and parallel inside a

module allows the output of a solar panel to be modified. The quantity of solar energy (in photons) entering a solar cell is proportional to the photocurrent I_{Ph} flowing through the cell.

The current drawn by a solar panel may be determined using Kirchoff's current law (KCL).

$$I_{PV} = I_{Ph} - I_D - I_{Rsh} \quad (1)$$

I_{Ph} is based on factors from the surrounding environment, including as irradiance and temperature. How to calculate your I_{Ph}:

$$I_{Ph} = \left(I_{sc} + \alpha\left(T_C - T_{ref}\right)\right)\frac{\lambda}{\lambda_{ref}} \quad (2)$$

The current through a diode is represented by the exponential function I_D.

$$I_D = I_s\left[\exp\left(\frac{q\left(V_{PV}+R_sI_{PV}\right)}{AkT_C}\right) - 1\right] \quad (3)$$

The relationship between temperature and the saturation current in a solar cell is exponential. A possible expression for I_s is

$$I_s = I_{Rs}\left(\frac{T_C}{T_{ref}}\right)^3 \exp\left[\frac{qE_g\left(\frac{1}{T_{ref}} - \frac{1}{TC}\right)}{KA}\right] \quad (4)$$

I_Rs is an exponential function that represents the saturation current flowing in the opposite direction.

$$I_{Rs} = \frac{I_{SC}}{\exp\left(\frac{qV_{OC}}{AkT_c}\right)-1} \quad (5)$$

As can be seen in Fig. 3, the shunt resistor current (I_{Rsh}) is calculated using Kirchoff's voltage law. The formula for I_{Rsh} is as follows:

$$I_{Rsh} = \frac{V_{PV}+R_sI_{PV}}{R_{sh}} \quad (6)$$

The defining characteristic of I_{PV} may be obtained by rewriting Eq. 1 as follows.

$$I_{PV} = I_{Ph} - I_s\left[\exp\left(\frac{q\left(V_{PV}+R_sI_{PV}\right)}{AkT_C}\right) - 1\right] - \frac{V_{PV}+R_sI_{PV}}{R_{sh}} \quad (7)$$

$$I_{Pv} = N_PI_{Ph} - N_pI_s\left[\exp\left(\frac{q\left(\frac{V_{PV}}{Ns}+\frac{R_SI_{PV}}{N_P}\right)}{AkT_C}\right) - 1\right] - \frac{\frac{N_PV_{PV}}{N_s}+R_sI_{PV}}{R_{Sh}} \quad (8)$$

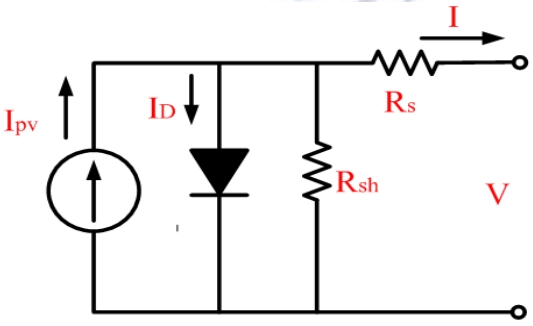

Fig 3. A PV cell's equivalent circuit

where,

I_{PV} : The output current of solar panel (A)
V_{PV} : The output voltage of solar panel (V)
I_{sc} : Short circuit current (A)
V_{oc} : Open circuit voltage (V)
α : Temperature coefficient ($V/°C$)
T_c : Solar panel temperature (K)
T_{ref} : Solar panel reference temperature (K)
λ : Irradiance (W/m^2)
λ_{ref} : Reference Irradiance ($W/m2$)
K : Boltzman's contant (1.38 × 10–23)
A : Ideality factor
q : Elementary charge (1.6 × 10–19 C)
E_g : Band gap energy of the semiconductor (eV)

B. Design of DC – DC Converter

The boost converter input is at the array's MPP voltage, or maximum power point. A voltage of 310 V may be calculated from this value. The boost converter's output voltage, or DC link voltage (Vdc), is kept constant at 400 V as the DC voltage that is to be supplied into the PMSM and then into VSI. Therefore, the duty ratio (D) of the converter might be established by,

$$D = \frac{V_{dc}-V_{PV}}{V_{dc}} = \frac{400-310}{400} = 0.225 \quad (9)$$

C. Design of Pump

The PMSM is coupled to a pump through a shaft when used for water pumping. According to the pump's torque speed characteristic, the load torque increases as the square of the motor's rotational velocity (ωr).

$$T_1 = K_P\omega_r^2 \quad (10)$$

$$k_P = \frac{T_1}{\omega_r^2} = \frac{10}{240.8^2} = 0.00017Nm/(rad/sec) \quad (11)$$

Where Kp is the pump constant and $\omega_r = \frac{N_r*\pi}{30}$ Nr is the rated motor speed.

4. CONTROL DESIGN OF PROPOSED SYSTEM CONFIGURATION

There are three primary methods through which the Fig. 1 topology may be modified. In this article, we will discuss the operation of MPPT, the generation of the reference speed and the modified speed error, and the regulation of the speed of a PMSM.

D. MPPT

This topology implements MPPT through an INC strategy. A maximum power point tracking (MPPT) method with INC control sets the operating point such that the instantaneous conductance is equal to the incremental conductance. Even in highly dynamic settings, MPP tracking speeds are assured. Due to its fast dynamic reactivity and anticipated lack of steady-state oscillation, it is particularly effective for solar water pumping. Figure 4 depicts the algorithm used by the INC MPPT method. For optimal static and dynamic performance, step size must be carefully considered. The step size used in this study is 0.01. The InC based MPPT method takes the PV array's current (Ipv) and voltage (Vpv) as inputs, and solves a series of governing equations, such as,

$$\Delta I_{PV} = I_{PV}(k) - I_{PV}(k-1) \quad (12)$$

$$\Delta V_{PV} = V_{PV}(k) - V_{PV}(k-1) \quad (13)$$

$$\frac{\Delta I_{PV}}{\Delta V_{PV}} = \frac{-I_{PV}}{V_{pv}}, \text{at MPP} \quad (14)$$

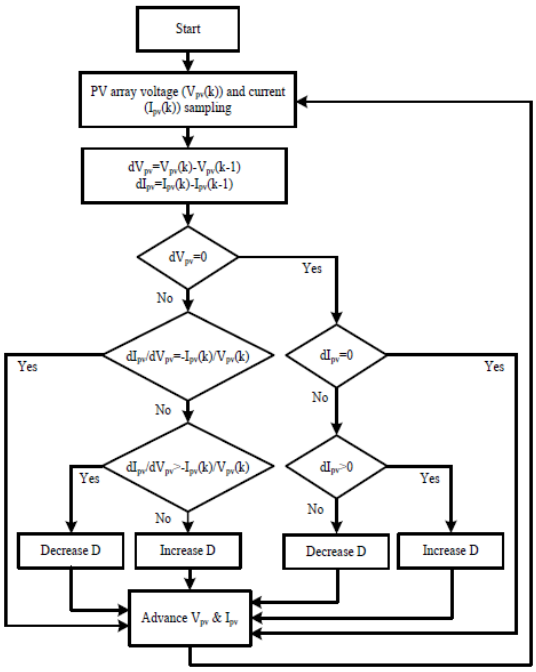

Fig. 4. INC MPPT algorithm.

$\frac{\Delta I_{PV}}{\Delta V_{PV}} > \frac{-I_{PV}}{V_{PV}}$, at Left of MPP on $P_{PV} - V_{PV}$ curve (15)

Where, P_{PV} is the PV array power

$\frac{\Delta I_{PV}}{\Delta V_{PV}} < \frac{-I_{PV}}{V_{PV}}$, at Right of MPP on $P_{PV} - V_{PV}$ curve (16)

An INC algorithm adjusts the duty ratio of the boost converter such that (9) is satisfied.

E. Generation of Reference Speed and Modified Speed Error

The described topology has a dual source of the reference speed (ω *). The DC link voltage controller provides the first half, while the feed-forward term from the solar PV system provides the second. In order to calculate the speed error (ωe*), is compared to the measured speed (ωr). To account for the system's non-linearities, we feed e and the rate of change in ωe (ωe) into an artificial neural network (ANN), which in turn produces a new speed error (ωe ANN) based on its own intelligence. The speed controller receives the total of the two errors, which is called the modified speed error (ωe mod). Error in DC link voltage at kth sample is defined as

$$V_{dce}(k) = V_{dc}^{*}(k) - V_{dC}(k) \quad (17)$$

The DC link voltage controller is fed the resulting voltage error. The DC link voltage controller makes adjustments to its output to reduce this mistake, which is then evaluated as ωk1*.

ω1* is expressed as,

$$\omega_1^{*}(k) = \omega_1^{*}(k-1) + K_{P\,dc}\{V_{dce}(k) - V_{dCe}(k-1)\} + K_{id}V_{dce}(k) \quad (18)$$

The DC link voltage controller makes use of the proportional constant Kpd and the integral constant Kid.

The PV power feed-forward term creates a ω2* (k) such that,

$$\omega_2^{*}(K) = k_{PV}P_{PV}(k) \quad (19)$$

Where, k_{PV} is solar PV feed forward constant.

The reference motor speed ω* is a sum of ω1* and ω2*.

$$\omega^{*}(k) = \omega_1^{*}(k) + \omega_2^{*}(k) \quad (20)$$

ω* (k) is compared to ωr (k) and the speed error is as,

$$\omega_e(k) = \omega^{*}(k) - \omega_r(k) \quad (21)$$

The rate of change in speed error is expressed as,

$$\Delta\omega_e(k) = \omega_e(k) - \omega_e(k-1) \quad (22)$$

F. Speed Control of PMSM

In this architecture, vector control is used to regulate transmission rates. After ωe mod has been generated, it is sent into the rate regulator. The current in the reference quadrature axis (Iq*) is taken from the output of the speed controller. The speed controller sets Iq* such that e mod is as close to zero as possible.

Iq* is expressed as,

$$I_q^{*}(K) = I_q^{*}(K-1) + K_{P\omega}\{\omega_{e\,mod}(k) - \omega_{e\,mod}(K-1)\} + k_{i\omega}\omega_{e\,mod}(k) \quad (23)$$

Where, Kpω and Kiω are proportional and integral constants, respectively utilized in speed controller.

No field weakening is required for solar water pumping since the pump speed must be maintained much below the base speed. Since this is the case, Id* is

always considered to be 0. From Id* and Iq*, the PMSM reference stator currents (ia*, ib*, and ic*) are derived using an inverse Park's transform (dq0 to abc). The detected motor phase currents ia, ib, and ic, as well as the reference currents ia*, ib*, and ic*, are fed to the hysteresis controller, which in turn generates the gating signals for VSI.

G.Proposed ANN Control

Artificial model of a neural network that behaves like a genuine one. Many of the "nodes" in an artificial neural network may stand in for individual brain cells. Neurons are able to communicate and interact with one another through these connections. Input data is taken in by nodes, and the processed data is then sent on to other nodes. The value or node that activates a node is the node's output. It is also believed that the links have a weight, and that this weight's variability affects the system's ability to learn. In the following image, you can see how speed error inputs are used in a simple ANN system. In this instance, the duty cycle value is trained with the speed error. These artificial neurons are trained to respond as approximated by a random function based on the data. Here, the duty cycle of the charge controller is predicted in response to varying irradiance and a constant temperature using a two-layer network. Throughout the training process, we used Levenberg-Marquardt back propagation. By controlling the duty cycle in this manner, the PMSM motor's output speed may be stabilised [18, 19].

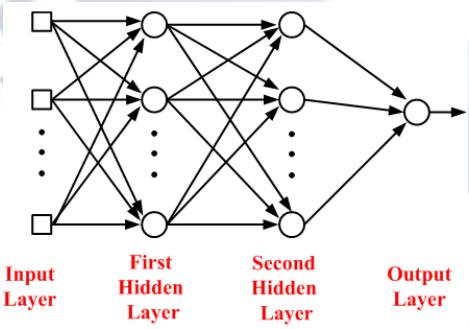

Fig .5 Schematic representation of ANN of Proposed System

5. Simulated Results

Using the Simscape sim power system toolbox in MATLAB/Simulink, we model a solar PV array-powered water pumping system that employs vector-controlled PMSM, and we verify its performance at startup, in steady state, and in dynamic settings like changing insolation and temperature. Starting and steady-state performance are represented combined for clarity, whereas dynamic performance is depicted independently. Variation in insolation (S), solar PV array voltage (Vpv), solar PV array current (Ipv), and solar PV array power (Ppv) are used to evaluate performance. Motor reference currents (iref), actual currents (iabc), modified speed error (e mod), reference and actual speeds (ref, r, respectively), and speeds (r) are all PMSM parameters. Switch voltage (vSW), switch current (iSW), diode voltage (vD), diode current (iD), duty ratio (D), and DC link voltage (Vdc) are all characteristics of a boost converter.

H. Starting and Steady State Performance

Figure 6 depicts the solar PV array and PMSM characteristics in both their beginning and final functioning phases. The solar PV characteristics may show a fast MPP tracking. The solar PV properties are stable in less than 0.01 s. It doesn't take long for iabc to start perfectly following iref, but r has to wait until it catches up since the speed control loop is often considerably slower than the current control loop. There is no other obvious issue with the solar PV and motor response metrics. The 400 V DC connection voltage has been maintained. The initial current draw from starting the engine is around 1.5 times the maximum continuous draw. In less than half a second, the motor's settings do not reach steady state values. Figure 6 is a graphical representation of the boost converter's parameters. The features of the boost converter also indicate a proper response.

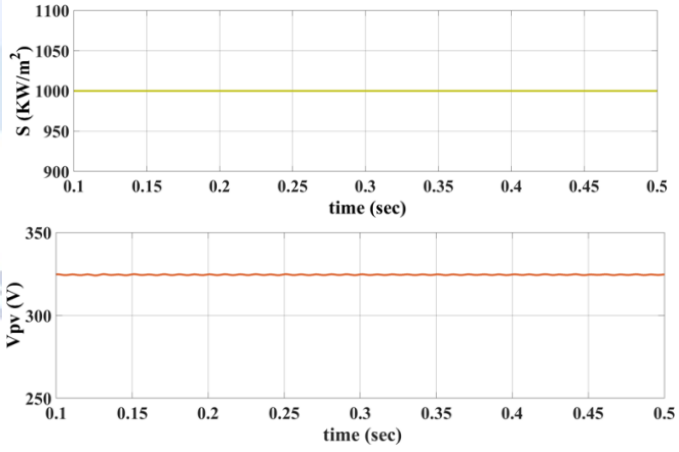

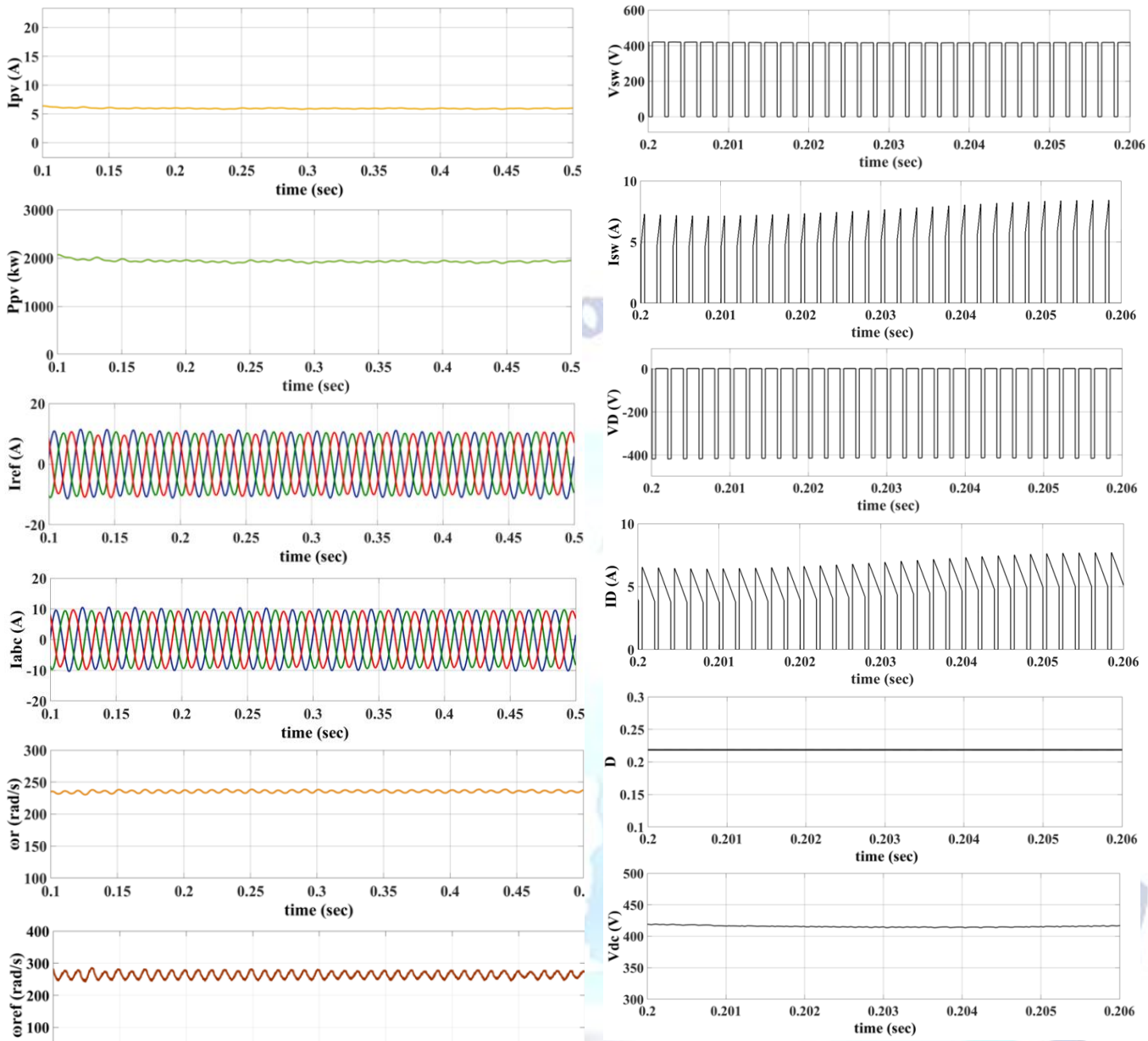

Fig.6. Performance metrics for solar photovoltaics (PVs), permanent magnet synchronous motors (PMSMs), and converters, both at startup and in steady state

I. Dynamic Performance under Changing Insolation

Using constant temperature and varying insolation, Figs. 7 displays the system's dynamic performance. For a decline in insolation from 1000 W/m2 to 500 W/m2 in 0.23 s, the response of the system parameters is shown in Fig. 6. However, we still keep the heat at a constant 250 degrees Celsius. There is no impact on Vpv from the change in insolation. However, it has a profound effect on Ipv. Since the amount of sunlight striking a PN junction is precisely equal to the number of free electrons created when a covalent bond is broken. Over half of the ipv has disappeared. As a consequence, the energy

produced by solar PV is cut by almost half. The motor settings adapt to the current situation. Less daylight means slower speeds and less torque. A new steady-state value for the insolation change is achieved in 0.23 s. Fig. 7 is a graphical representation of the impact of a 500 W/m2 to 1000 W/m2 increase in insolation. When going from 500 W/m2 of sunshine to 1000 W/m2, the system's efficiency begins to flip.

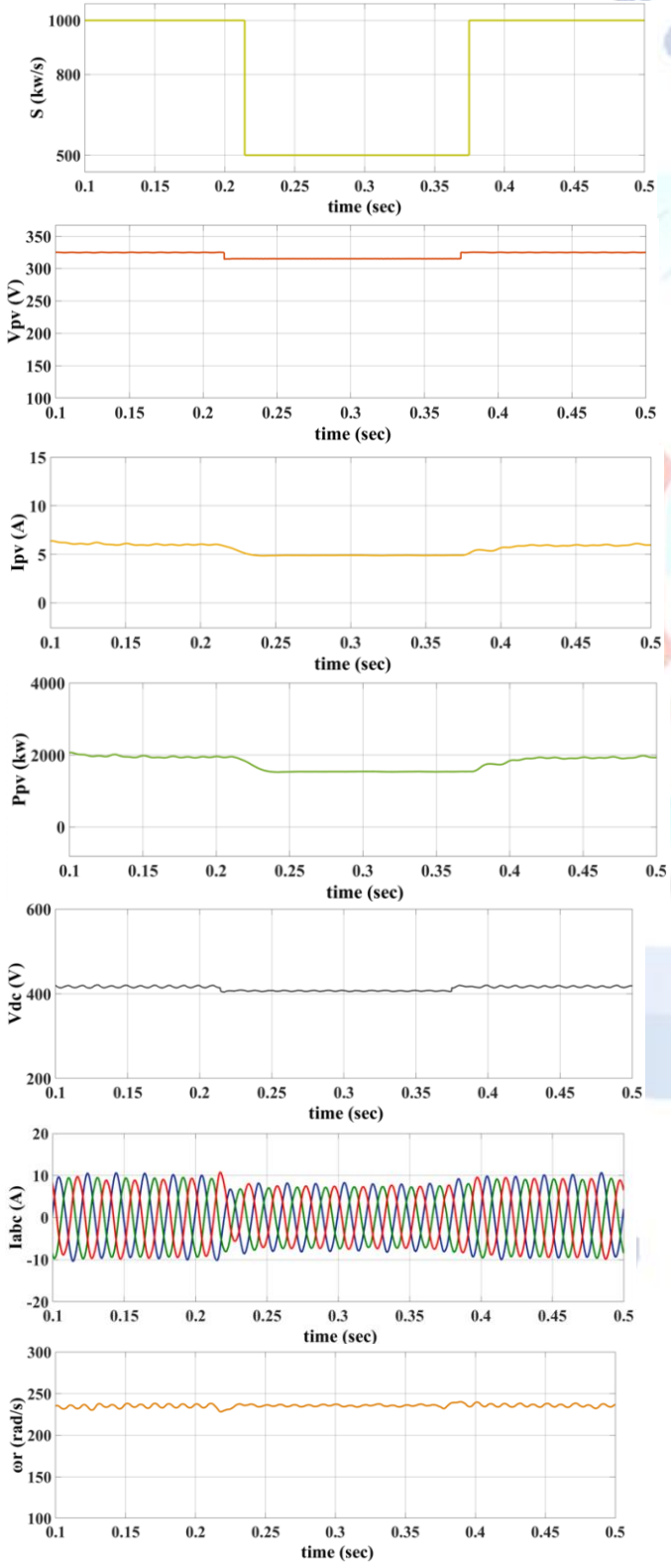

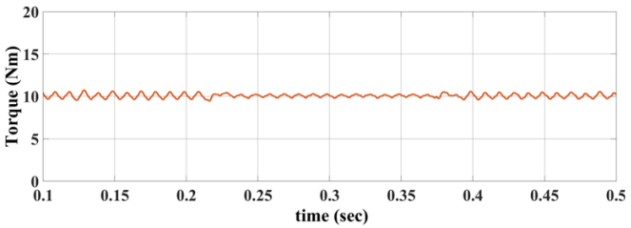

Fig.7 Adaptability to changes in insolation, from 1000 W/m2 to 500 W/m2 and back again.

6. Conclusion

In conclusion, using Artificial Neural Networks (ANNs) to regulate PMSM motors in solar water pumping systems is promising and beneficial. The study shows various advantages of this technique. ANNs have shown they can boost PMSM drive efficiency in solar water pumping. ANNs optimise water production and energy usage by fine-tuning motor control settings in real time depending on environmental variables and load needs. In rural or off-grid places, solar water pumping systems must be sustainable and cost-effective. A major benefit of ANNs is their versatility. Solar irradiance and weather affect solar-powered systems. ANNs can automatically modify control techniques to these changes, delivering consistent and dependable performance throughout the day and under different conditions. System resilience is enhanced via adaptation. ANNs can forecast and reduce PMSM drive problems, improving system dependability. This predictive capacity may save expensive downtime and assure water supply in distant or inaccessible sites where maintenance and repairs are difficult. The use of Artificial Neural Networks to regulate PMSM motors for solar water pumping systems is a step towards sustainable and efficient water delivery. This research shows that ANNs may make solar water pumping systems more energy-efficient, adaptive, and dependable, solving global water supply issues.

Conflict of interest statement

Authors declare that they do not have any conflict of interest.

References

[1] K. Yoshikawa, H. Kawasaki, W. Yoshida, T. Irie, K. Konishi, K. Nakano, T. Uto, D. Adachi, M. Kanematsu, H. Uzu and K. Yamamoto, "Silicon heterojunction solar cell

with interdigitated back contacts for a photoconversion efficiency over 26%," Nature Energy, vol.2, no. 5, Mar. 2017, Art. no. 17032.

[2] A. Aggarwal, A. Singhal and S. J. Darak, "Clean and Green India: Is Solar Energy the Answer," IEEE Potentials, vol. 37, no. 1, pp. 40-46, Jan.-Feb. 2018.

[3] S. Shukla and B. Singh, "Single-Stage PV Array Fed Speed Sensorless Vector Control of Induction Motor Drive for Water Pumping," IEEE Trans. Ind. Appl., vol. 54, no. 4, pp. 3575-3585, July-Aug. 2018.

[4] M. Rezkallah, A. Chandra, M. Tremblay and H. Ibrahim, "Experimental implementation of an APC with enhanced mppt for standalone solar photovoltaic based water pumping station," IEEE Trans. Sust. Energy, vol vol. 10, no. 1, pp. 181-191, Jan. 2019.

[5] M. Kolhe, J. C. Joshi and D. P. Kothari, "Performance analysis of a directly coupled photovoltaic water-pumping system," IEEE Trans. Energy Conv., vol. 19, no. 3, pp. 613-618, Sept. 2004.

[6] J. V. M. Caracas, G. d. C. Farias, L. F. M. Teixeira and L. A. d. S. Ribeiro, "Implementation of a High-Efficiency, High-Lifetime, and Low-Cost Converter for an Autonomous Photovoltaic Water Pumping System," IEEE Trans. Ind. Appl., vol. 50, no. 1, pp. 631-641, Jan.-Feb. 2014.

[7] B. Singh and S. Murshid, "A Grid-Interactive Permanent-Magnet Synchronous Motor-Driven Solar Water-Pumping System," IEEE Trans. Ind. Appl., vol. 54, no. 5, pp. 5549-5561, Sept.-Oct. 2018.

[8] T. Brinner, R. H. McCoy and T. Kopecky, "Induction versus permanent-magnet motors for electric submersible pump field and laboratory comparisons," IEEE Trans. Ind. Appl., vol. 50, no. 1, pp. 174-181, 2014.

[9] A. K. Mishra and B. Singh, "Solar Photovoltaic Array Dependent Dual Output Converter Based Water Pumping Using Switched Reluctance motor Drive," IEEE Trans. Ind. Appl., vol. 53, no. 6, pp. 5615-5623, Nov.-Dec. 2017.

[10] R. Kumar and B. Singh, "BLDC Motor-Driven Solar PV Array-Fed Water Pumping System Employing Zeta Converter," IEEE Trans. Ind. Appl., vol. 52, no. 3, pp. 2315-2322, May-June 2016.

[11] R. Krishnan, "Permanent Magnet Synchronous and Brushless DC Motor Drives," 1st Ed., Boca Raton, Florida, FL, USA, CRC Press, 2010.

[12] A. Shinohara, Y. Inoue, S. Morimoto and M. Sanada, "Maximum Torque Per Ampere Control in Stator Flux Linkage Synchronous Frame for DTC-Based PMSM Drives Without Using q-Axis Inductance," IEEE Trans. Ind. Appl., vol. 53, no. 4, pp. 3663-3671, July-Aug. 2017.

[13] P. Pillay and R. Krishnan, "Modeling, simulation, and analysis of permanent-magnet motor drives. I. The permanent-magnet synchronous motor drive," IEEE Trans. Ind. Appl., vol. 25, no. 2, pp. 265-273, March-April 1989.

[14] D. Liang, J. Li and R. Qu, "Sensorless Control of Permanent Magnet Synchronous Machine Based on Second-Order Sliding-Mode Observer With Online Resistance Estimation," IEEE Trans. Ind. Appl., vol. 53, no. 4, pp. 3672-3682, July-Aug. 2017.

[15] M. A. Hannan, J. A. Ali, A. Mohamed, U. A. U. Amirulddin, N. M. L. Tan and M. N. Uddin, "Quantum-Behaved Lightning Search Algorithm to Improve Indirect Field-Oriented Fuzzy-PI Control for IM Drive," IEEE Trans. Ind. Appl., vol. 54, no. 4, pp. 3793-3805, July-Aug. 2018.

[16] S. Murshid and B. Singh, "Simulation and hardware implementation of PMSM driven solar water pumping system," in proc. Int. Conf. on Pow., Inst., Ctrl. and Comp. (PICC), Thrissur, 2018, pp. 1-6.

[17] Y. Lee and S. Sul, "Model-Based Sensorless Control of an IPMSM With Enhanced Robustness Against Load Disturbances Based on Position and Speed Estimator Using a Speed Error," IEEE Trans. Ind. Appl., vol. 54, no. 2, pp. 1448-1459, March-April 2018.

[18] D. Bao, X. Pan, Y. Wang, X. Wang and K. Li, "Adaptive Synchronous-Frequency Tracking-Mode Observer for the Sensorless Control of a Surface PMSM," IEEE Trans. Ind. Appl., vol. 54, no. 6, pp. 6460-6471, Nov.-Dec. 2018.

[19] L. Sheng, G. Xiaojie and Z. Lanyong, "Robust Adaptive Backstepping Sliding Mode Control for Six-Phase Permanent Magnet Synchronous Motor Using Recurrent Wavelet Fuzzy Neural Network," IEEE Access, vol. 5, pp. 14502-14515, 2017.

[20] B. Subudhi and R. Pradhan, "A Comparative Study on Maximum Power Point Tracking Techniques for Photovoltaic Power Systems," IEEE Trans. Sust. Energy, vol. 4, no. 1, pp. 89-98, Jan. 2013.

[21] Sunmodule-SW250 Standard Solar PV Module Specifications[Online].https://www.solarworldusa.com/~/media/www/files/datasheets/sunmodule-plus/sunmodule-solar-panel-250-mono-ds.pdf

[22] M.Kaliamoorthy, R.M.Sekar, I. Gerald Christopher Raj, "Solar Powered Single Stage Boost Inverter with ANN Based MPPT Algorithm," 2010 IEEE International Conference on Communication Control and Computing Technologies (ICCCCT).

[23] R.Ramaprabha1, B.L.Mathur and M.Sharanya, "Neural-Network-Based Maximum-Power-Point Tracking of Coupled-Inductor Interleaved-Boost-Converter-Supplied PV System Using Fuzzy Controller," Proceedings of International Conference on Control, Automation, Communication and Energy Conservation.